

5 *Spatial Array Measurements and Experimental Procedure*

I don't like to read books; they muss up my mind.

Henry Ford

5.1 Introduction

Extracting the desired information from a seismic wavefield offers several practical challenges. Spatial inhomogeneities of material properties, array imperfections, seismic noise statistical properties, sensor and equipment electrical noise, and wave propagation multipath and diffraction all interfere with the measurement process. Digital sampling of a natural process offers several drawbacks that cause imperfection in experimental measurements. Some practical difficulties include: 1.) Signals are rarely perfectly bandlimited, 2.) To represent signals of infinite extent, an infinite number of samples are required, and 3.) Digital samples are only accurate to a finite number of bits (Johnson and Dudgeon, 1993).

5.2 Data Acquisition Equipment and System Control

The typical data acquisition configuration includes a Hewlett-Packard (HP) VXI system, 16 sensors, a signal conditioner, and external monitor. The system control software was written in Matlab, and allows in-field control of digital signal processing and spatial array properties. Figure 5.1 shows the data acquisition equipment and setup.

5.2.1 VXI Mainframe Data Acquisition System and Signal Conditioning

The HP VXI mainframe case contains an embedded 133 MHz Pentium controller, including 32 MB DRAM, an A/D converter and dynamic signal analyzing module, and an HP E1562D throughput module. The Pentium controller allows programming of the dynamic signal analyzer through Matlab in a Windows NT environment. The 16 channel, 16 bit HP E1432A digitizer plus dynamic signal processor allows sampling of each channel

at up to 51.2 kSamples/sec. A PCB Piezotronics 440 module provides signal conditioning and selectable gains of 1, 10, and 100 for the low noise ICP seismic accelerometers. The module contains four 4 channel PCB 442A104 signal conditioners.

5.2.2 Sensors and Cables

High sensitivity and resolution are the primary requirements of seismic sensors. Two types of sensors were used in the experimental results presented in this dissertation. Each sensor is discussed briefly, giving the primary characteristics of interest. For the typical frequencies of seismic interest, the loss of signal quality due to driving long cables is not a factor.

5.2.2.1 Wilcoxon Research 731A Seismic Accelerometer

The Wilcoxon Research 731A Ultra-Quiet, Ultra Low Frequency seismic accelerometer provides a flat frequency response between 0.2 Hz and 100 Hz, with a resonance frequency near 950 Hz, and a typical sensitivity of 10 V/g. The sixteen 731A sensors used in spatial array measurements have sensitivities varying from 9.4 to 10.6 V/g. The ease of calibration and robustness of the accelerometers are advantageous for increased confidence in attenuation measurements. Wilcoxon low noise, R1-2-J93 coaxial cables were used in all measurements.

5.2.2.2 Mark Products L4-C Geophone

For the active surface wave tests presented in Chapters 6 and 7, Mark Products Model L4-C geophones, with a natural frequency of 1 Hz and mass of 981 grams, were used. The geophones measure vertical particle motion and have a typical sensitivity of 10 to 13 Volts/(in/sec). An advantage of the geophones is that they do not need an electrical source, since movement of the mass induces a voltage in a surrounding electrical coil.

5.2.3 Seismic Surface Wave Sources

The characteristics of different seismic surface wave sources differ significantly, in terms of frequency range and power. Passive sources tend to propagate with lower frequencies, and therefore, longer wavelengths, but have more restrictive stationarity requirements compared to active sources. Impulsive and harmonic active sources offer more control over the seismic wavefield, but differ in their specific advantages and disadvantages. This section gives a brief overview of seismic surface wave sources, and when required, specific source details pertaining to experimental results will be discussed in Chapters 6 to 8.

Two types of active surface wave sources have traditionally been employed. Impulsive sources, such as hammers, buckets, and dropped weights, represent the most commonly used active source in geotechnical surface wave tests. Different impact sources generate usable input energy over different frequency ranges (Spang, 1995). The major advantage of impulsive sources is the ability to stack time domain measurements to increase signal to noise ratios.



Figure 5.1 Data Acquisition System

Harmonic or continuous sources allow more control over the frequency range in which usable energy is generated. A significant advantage of harmonic sources is the ability to generate meaningful energy content at lower frequencies than impulsive sources (Spang, 1995). In traditional surface wave testing, the experimental measurements of harmonic source wavefields have been averaged in the spectral domain, and therefore, the variance of the power estimate has been reduced but not noise power. The ideal surface wave source would be harmonic source measurements stacked in the temporal domain to remove noise before estimating the power spectrum.

For active test results presented in Chapters 6 and 7, an APS Dynamics, Inc. Model 400 Electro-Seis Shaker was used to create the active surface wavefield. The shaker can be operated in sinusoidal and random excitation modes, with frequencies ranging from less than 1 Hz to 200 Hz. Typical measurements span 5 Hz to 100 Hz, due to the difficulty of imparting enough energy into the ground to measure surface waves at very low frequencies. A detailed review of the characteristics and power output abilities of the shaker can be found in Spang (1995).

Passive seismic surface wave sources include cultural noise, such as construction activity, microtremors, and traffic energy. Passive sources are classified as either long-period (1 to 5 seconds) or short-period (less than 1 second) (Tokimatsu, 1995) and have two properties which are advantageous for surface wave tests. First, passive sources create measurable energy at frequencies lower than those typically produced by active sources.

Second, passive sources are typically measured in the far-field, allowing valid recourse to the plane wave assumption. The first advantage allows the dynamic properties of soil profiles to be estimated to larger depths, while the plane wave nature of passive waves is important for material attenuation estimates.

Analysis of passive surface sources also introduces several complications. First, passive sources are only statistically stationary over a finite time length. In comparison, active sources yield repeatable source statistics, allowing use of synthetic linear arrays as discussed in Chapter 6. Second, typical passive sources, such as microtremors and traffic energy, exhibit nonstationary source locations and directions of arrival as a function of time and frequency. A changing source location affects the estimation of the spatio-spectral matrix, especially when multiple modes are present. For more detailed discussions of passive sources and ambient seismic noise, see Tokimatsu (1995), Aki and Richards (1980), and Frantti, et al. (1962).

5.2.4 System Control Software

System control software written in Matlab allows input of spatial array and digital signal processing parameters. The necessary parameters include sampling frequency, number of blocks of data to be averaged, block length, and sensor vector locations. The software allows analysis and viewing of array spectral characteristics before making measurements. Additionally, any changes in placement of sensor locations can be easily altered in the software if a sensor cannot be placed exactly as designed. During measurements, the output of individual sensors can be viewed. After measurements, the

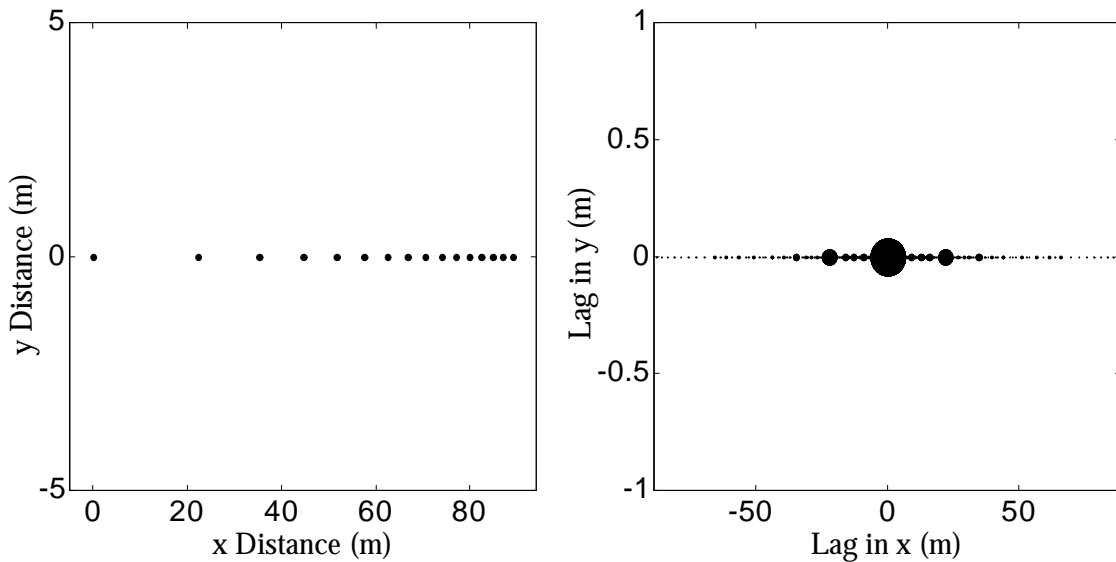


Figure 5.2 Sixteen Sensor Non-Uniform Linear Array. The array geometry (left panel) and coarray (right panel) are shown.

frequency-wavenumber power spectrum can be estimated for selected frequencies to check results in the field.

5.3 Array Comparisons

The array smoothing function must be explicitly analyzed to determine the array geometry with the best properties for a given problem. The spectral properties depend directly on the coarray, and although sometimes the most efficient array is one with a regular underlying grid, usually arrays with good coverage of spatial lags in the coarray are desired. The present section will consider and compare several array geometries, their coarrays, and their array smoothing functions. The chosen arrays, along with the previously presented arrays in Chapter 4, will help crystallize some of the main concerns, i.e. aliasing,

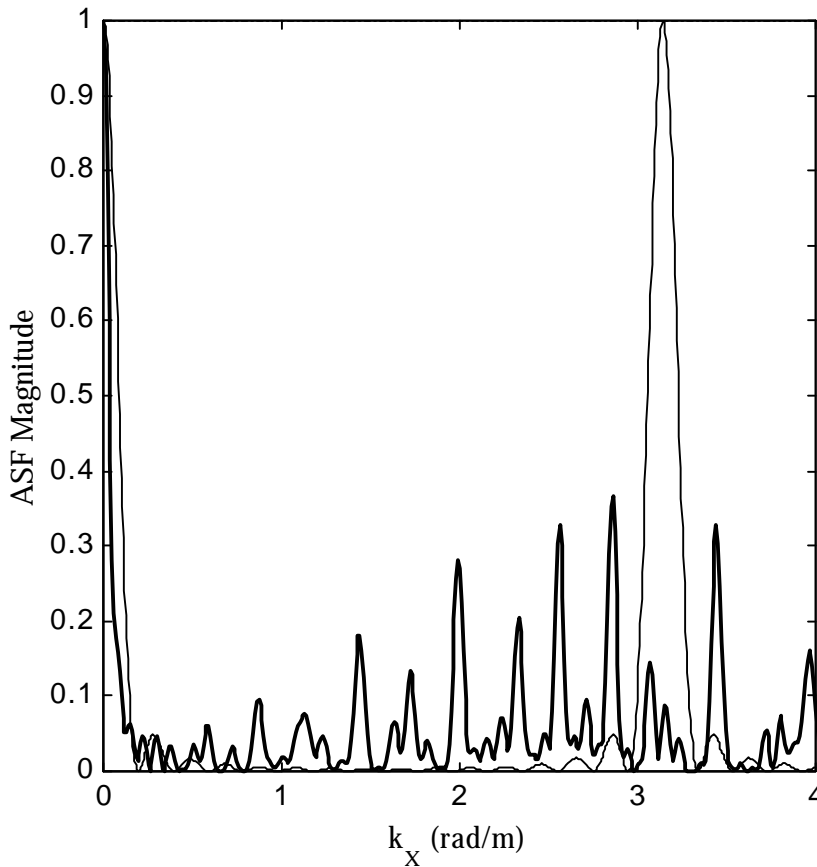


Figure 5.3 Comparison of Non-Uniform and Uniform Linear Array Spectral Characteristics. The non-uniform linear array (dark line) and uniform linear array (light line) smoothing functions are shown. Notice the increased resolution, measured by the narrower mainlobe width, and the increased sidelobe heights of the non-uniform linear array compared to the uniform linear array.

resolution, and energy leakage, to consider when designing arrays for field testing. The arrays used in previous studies of geotechnical interest, i.e. the circular array implemented by Tokimatsu (1995) and the L-shaped array implemented by Horike (1985), will also be considered.

5.3.1 Sixteen Sensor Non-Uniform Linear Array

Figure 5.2 shows a non-uniformly spaced sixteen sensor array and coarray. The minimum sensor separation d_{\min} equals 2 m and the total array length, or maximum spatial lag, equals 89.1 m. The non-uniform spacing of the sensors yields more coverage of the coarray than the uniform linear array introduced in Figure 4.7. The uniform linear array introduced in Figure 4.7 has the same minimum sensor separation $d_{\min} = 2$ m, but the total array length is only 30 m. Figure 5.3 shows the array smoothing functions for both the non-uniform (dark line) and uniform (light line) linear arrays.

Several important spectral features regarding the array smoothing functions should be emphasized. First, recall that the uniform spacing of samples for the uniform linear array led to the presence of a strong grating or aliasing lobe. The non-uniform linear array, on the other hand, does not exhibit the grating lobe due to the irregular sampling of the spatial domain. Inspecting the mainlobe width of the two array smoothing functions, the non-uniform array has a narrower mainlobe due to the longer total array length. In return for the increase in resolution, the non-uniform array's ability to control energy leakage has diminished significantly, which is seen in the increased sidelobe heights compared to the uniform linear array.

5.3.2 Six Sensor Perfect Array

Array geometries can be chosen to minimize the number of redundant spatial lag samples. An array with no redundant lags, other than the zero lag, on a regular grid are called perfect arrays (Johnson and Dudgeon, 1993). Figure 5.4 shows a six sensor, two-dimensional array and its coarray. Notice the coarray has no redundant lags other than the zero lag. Figure 5.5 shows the array smoothing function. The regular underlying sampling grid leads to easily identified grating lobes and a regular array smoothing function

5.3.3 Five Sensor Circular Array with Center Sensor

The earliest array applied directly to geotechnical near surface earth site characterization was a five sensor circular array with an additional center sensor (Tokimatsu, 1995). Figure 5.6 shows the array and coarray for a circle of radius = 10 m, and Figure 5.7 shows the spectral properties of the array. Since only six sensors are used, the spectral leakage properties of the array are not ideal. As seen in the right panel of Figure 5.7, the approximate aliasing criteria in the y-direction, about $k_y = 0.3$ rad/m, based on the very large sidelobe at about $k_y = 0.6$ rad/m, and the resolution criteria in the y-direction, about 0.25 rad/m, are almost identical. The poor array spectral properties are due to the limited number of samples. The results from using the array have been successful (Tokimatsu, 1995), especially when a single, identifiable source has been used, but the array smoothing function displays poor filtering characteristics.

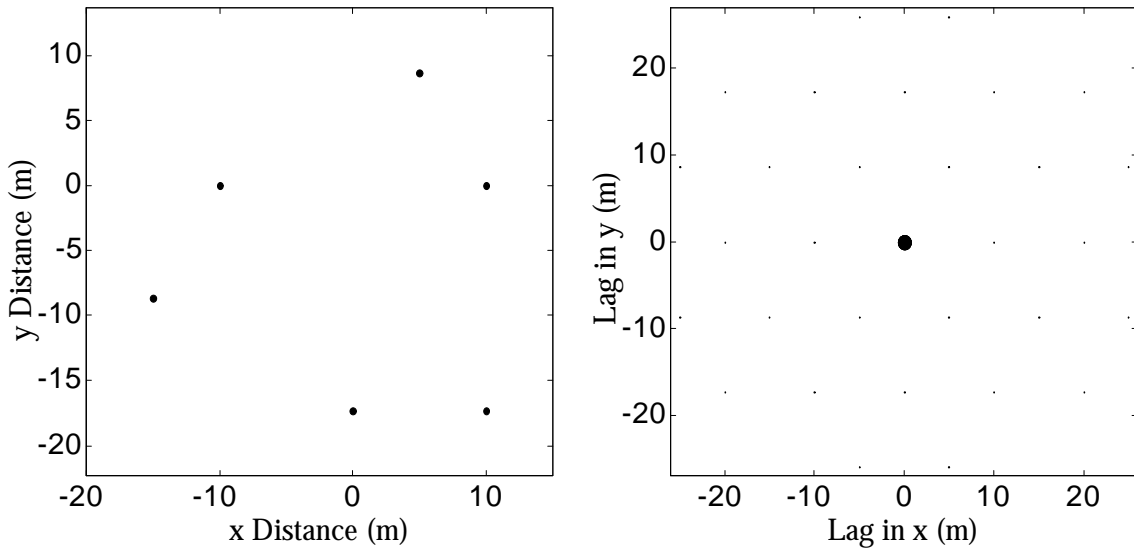


Figure 5.4 Perfect Six Sensor Two-Dimensional Array. The array geometry is shown in the left panel and the coarray is shown in the right panel.

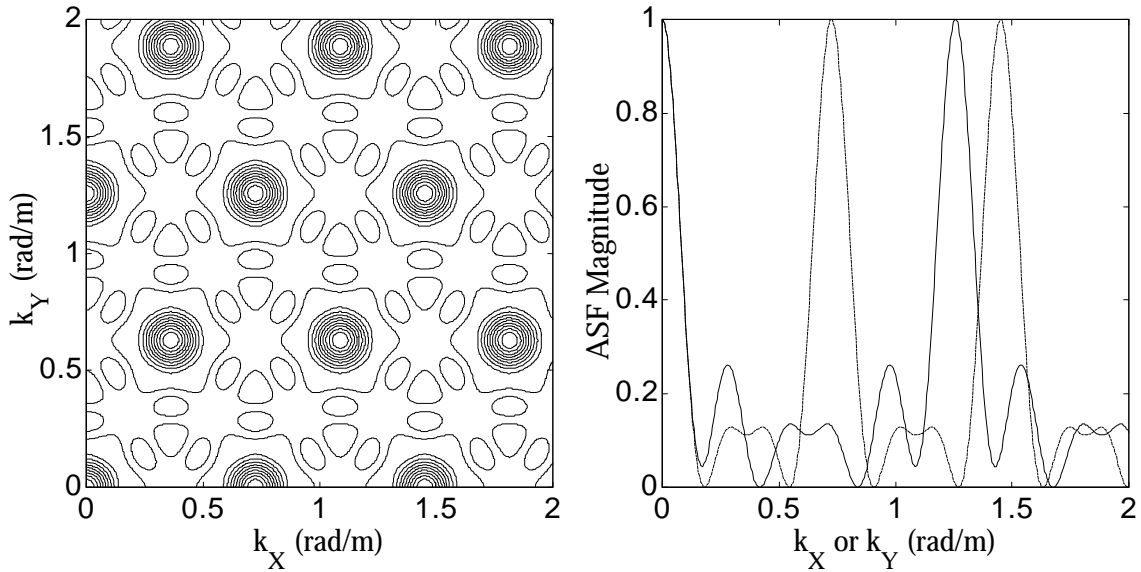


Figure 5.5 Perfect Six Sensor Array Spectral Characteristics. The array smoothing function (left panel) and orthogonal slices (right panel) along the k_x -axis (dashed line) and k_y -axis (solid line) for the two-dimensional perfect array from Figure 5.4 are shown.

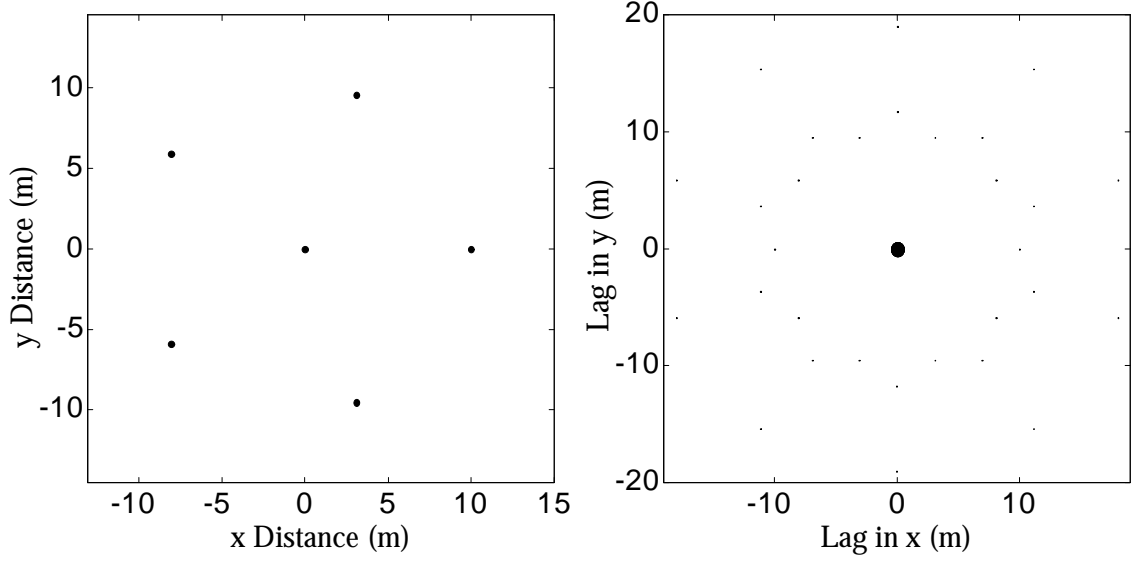


Figure 5.7 Five Sensor Circular Array with a Center Sensor (left panel) and Coarray

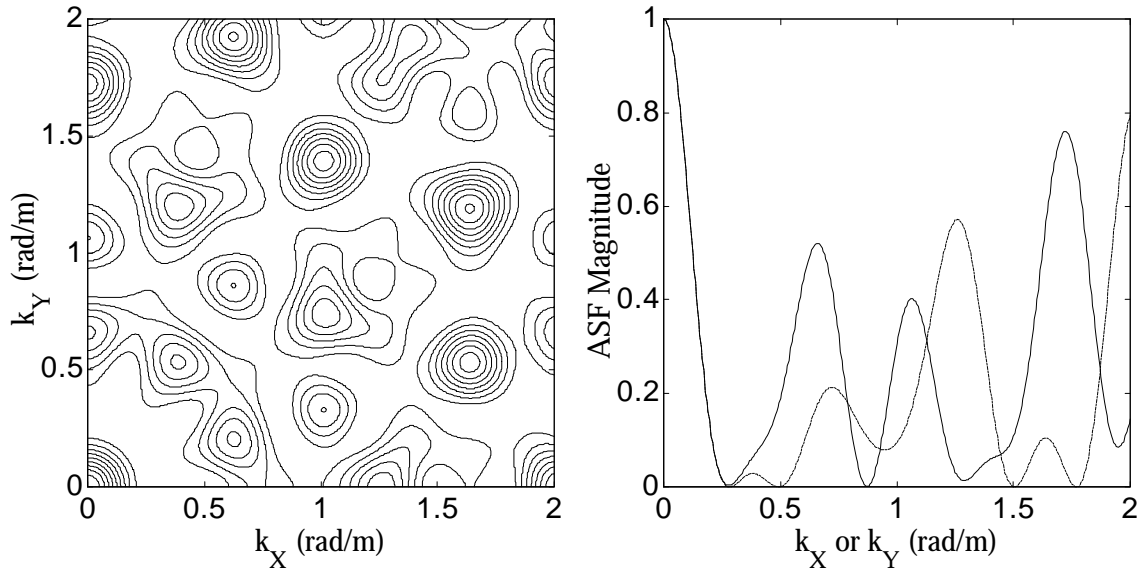


Figure 5.6 The Array Smoothing Function for the Five Sensor Circular Array with a Center Sensor. The array smoothing function (left panel) and orthogonal slices (right panel) along the k_x -axis (dashed line) and k_y -axis (solid line) are shown for the array from Figure 5.6.

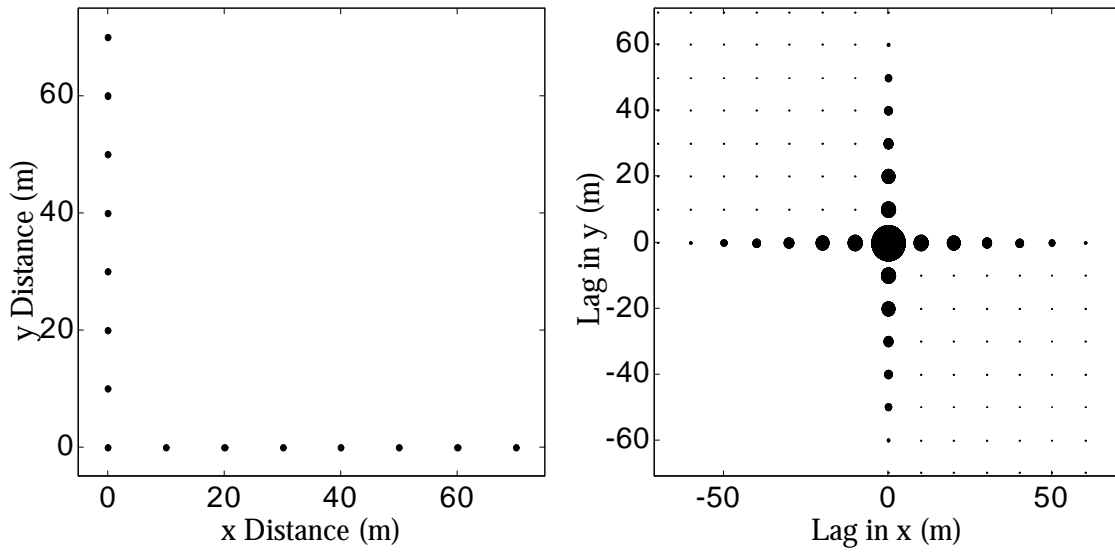


Figure 5.8 Fifteen Sensor L-shaped Array (left panel) and Coarray (right panel)

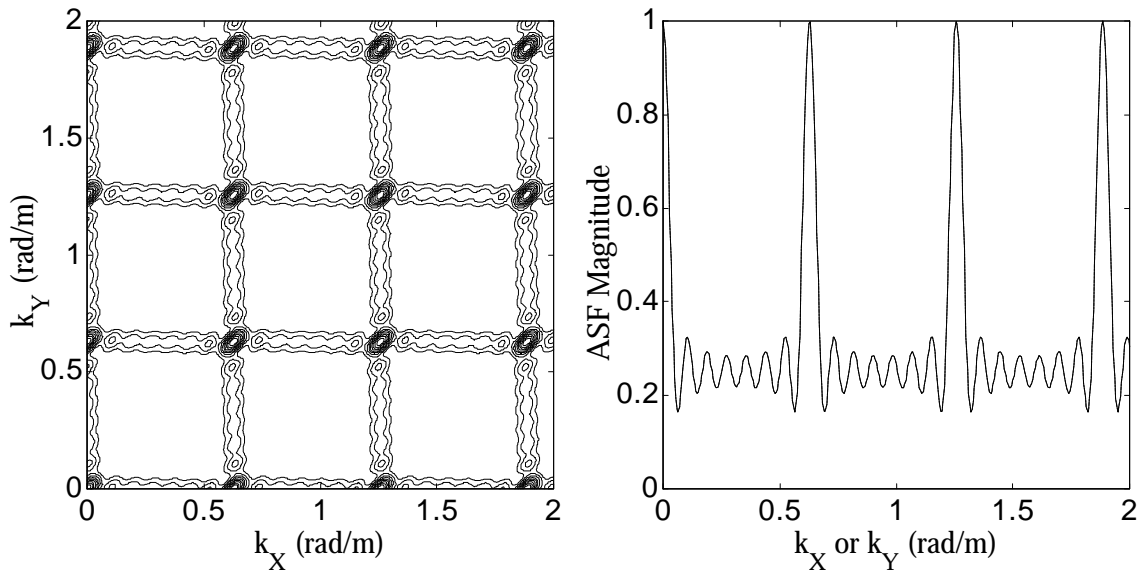


Figure 5.9 Spectral Properties of an L-Shaped Array. Array smoothing function (left panel) and slices (right panel) along the k_x -axis and k_y -axis (solid line), which are equivalent, are shown for the L-shaped array shown in Figure 5.8.

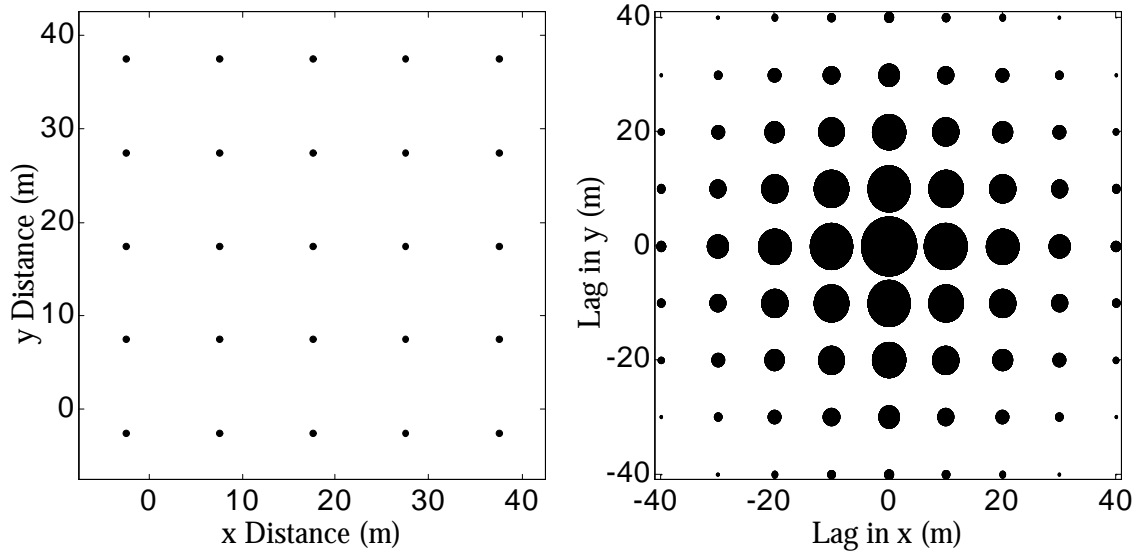


Figure 5.10 Sixteen Sensor Square Array (left panel) and Coarray (right panel)

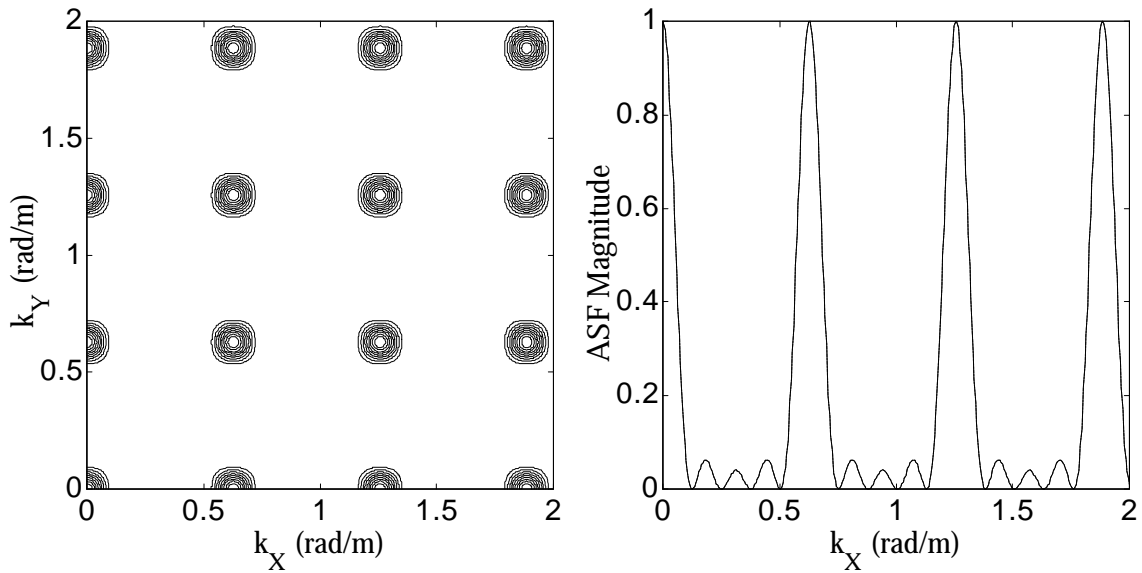


Figure 5.11 Spectral Characteristics of Square Array. The array smoothing function (left panel) and slice (right panel) along the k_x -axis are shown for the 16 sensor square array in Figure 5.10.

5.3.4 Fifteen Sensor L-Array

Non-symmetric sampling of spatial lags will lead to preferential directions in the array smoothing function. The left panel of Figure 5.8 shows a 15 sensor L-shaped array, with sensor separation equal to 10 m along each axis, similar to the L-shaped array geometry used by Horike (1985). The right panel of Figure 5.8 shows the coarray. Notice the axisymmetric sampling of the coarray, which leads to an ellipse shaped mainlobe in the array smoothing function, shown in the left panel of Figure 5.9. Therefore, the array displays different resolution for waves propagating from a 45 degree angle than for waves propagating from a 0 or 90 degree angle, as measured from the x-axis.

5.3.5 Sixteen Sensor Square Array

Regular sampling in both the x and y-directions yields array smoothing functions with sharp aliasing criteria. Figure 5.10 shows a 16 sensor dense square array and coarray. Similar to a uniform linear array, the coarray shows a great deal of lag redundancy. Figure 5.11 shows the array smoothing function. The square array displays sharp grating lobes, allowing easy recognition of aliasing criteria.

5.4 Array Choice

In early array tests conducted in this study, experimental measurements of passive surface waves were conducted with several different array geometries. Sixteen sensor circular arrays without a center sensor were chosen for the following reasons: 1.) The array appears to have almost the same dimensions for a plane wave impinging from any direction, 2.) The symmetry of the underlying array smoothing function allows identification of maximum wavenumber before encountering large sidelobes, and 3.) The array shows good resolution characteristics.

5.5 Summary

Although the theory of spatial array and digital signal processing is well understood, practical implementation encounters several conditions differing from the ideal situation. Limited equipment and the nature of finite precision digital sampling force engineering estimates to be made from limited and imperfect data. In most cases, the finite precision of digital samplers is not detrimental, but in cases with small signal-to-noise ratios, the finite precision affects the ability to resolve signal from noise.

The limited number of sensors drastically inhibits the ability to adequately measure a two-dimensional spatial wavefield. Compared to the one-dimensional temporal case, in which retrieving an additional time sample is relatively inexpensive, an additional spatial data sample requires an additional acquisition channel and the deployment of an additional sensor. Therefore, the design of effective array geometries is imperative to maximize the information content of spatial array measurements. To determine the best sensor design for passive surface wave measurements, several array geometries, including a few of the array designs previously used in geotechnical studies, and their underlying spectral characteristics were discussed. The sixteen sensor circular array was chosen due to the symmetry and easily analyzable spectral characteristics. Experimental results using the 16 sensor circular array are presented in Chapter 8.